

# Soft 3D acoustic metamaterial with negative index

Thomas Brunet<sup>1\*</sup>, Aurore Merlin<sup>2</sup>, Benoit Mascaro<sup>1</sup>, Kevin Zimny<sup>2</sup>, Jacques Leng<sup>3</sup>, Olivier Poncelet<sup>1</sup>, Christophe Aristégui<sup>1</sup> and Olivier Mondain-Monval<sup>2</sup>

**Many efforts have been devoted to the design and achievement of negative-refractive-index metamaterials since the 2000s<sup>1–8</sup>. One of the challenges at present is to extend that field beyond electromagnetism by realizing three-dimensional (3D) media with negative acoustic indices<sup>9</sup>. We report a new class of locally resonant ultrasonic metafluids consisting of a concentrated suspension of macroporous microbeads engineered using soft-matter techniques. The propagation of Gaussian pulses within these random distributions of ‘ultra-slow’ Mie resonators is investigated through *in situ* ultrasonic experiments. The real part of the acoustic index is shown to be negative (up to almost  $-1$ ) over broad frequency bandwidths, depending on the volume fraction of the microbeads as predicted by multiple-scattering calculations. These soft 3D acoustic metamaterials open the way for key applications such as sub-wavelength imaging and transformation acoustics, which require the production of acoustic devices with negative or zero-valued indices.**

Unlike periodic structures—that is, photonic crystals for light<sup>2</sup> or phononic crystals for sound<sup>3</sup>, in which negative refraction is a consequence of band-folding effects—the negative index of a metamaterial originates from low-frequency resonances of sub-wavelength particles. A negative refractive index in electromagnetism was first experimentally verified at microwave frequencies<sup>4</sup>; since then, other experimental demonstrations of negative-index metamaterials have been reported in the near-infrared domain<sup>5,6</sup> and at optical wavelengths<sup>7</sup>. However, the metamaterial concept applies not only to electromagnetism<sup>8</sup> but also to different fields such as acoustics<sup>9</sup>. Since the first experimental realization of ‘locally resonant sonic materials’<sup>10</sup>, negative-acoustic-index metamaterials have been achieved only for the audible domain through the use of two-dimensional solid structures consisting of periodic arrays of interspaced membranes and side holes<sup>11</sup> or arrays of Helmholtz and rod–spring resonators<sup>12</sup>. Coiling up space has also proved to be an effective method for providing acoustic metamaterials with extreme constitutive parameters<sup>13,14</sup>. Possible future applications such as perfect acoustic lenses, by analogy with John Pendry’s perfect electromagnetic lens<sup>15</sup>, call for 3D negative-acoustic-index metamaterials, which have not yet been achieved<sup>16</sup>.

Unlike the mechanical engineering techniques that are usually applied to machine 1D (ref. 17) or 2D (ref. 18) solid structures, soft-matter techniques are very promising for the fabrication of metamaterials because they should yield 3D locally resonant metafluids, or so-called soft acoustic metamaterials<sup>19</sup>, which present the following advantages: macroscopic isotropy, unlike the most general class of acoustic metafluids with anisotropic inertia<sup>20,21</sup>; broad versatility, as microfluidics<sup>22</sup> allows the up-scaled production

of micro-resonators with controlled sizes, shapes and compositions; potential tunability, as soft inclusions can be either deformed or oriented under external stimuli<sup>23</sup>; and facile shaping and moulding, as the host matrix is fluid.

A unique method of achieving 3D negative-acoustic-index metamaterials is to benefit from strong low-frequency Mie resonances (monopolar and dipolar) of ‘ultra-slow’ inclusions<sup>24</sup>. However, no dense homogeneous material possesses a sufficiently low sound speed to exhibit such a feature, not even the so-called ‘soft silicone rubbers’<sup>25</sup>. By contrast, the use of porous soft silicone rubbers should be more promising because the sound speed in porous media is very low<sup>26</sup>, with the latter depending on the ratio between the elastic moduli and mass density. Indeed, the large volume of air cavities present in porous materials causes them to be very soft (or highly compressible), thereby allowing these materials to exhibit very low elastic moduli while maintaining relatively high mass densities because of their solid skeletons. Particles composed of such ‘ultra-slow’ materials ( $v_1 \approx 100 \text{ m s}^{-1}$ ) randomly dispersed in water ( $v_0 \approx 1,500 \text{ m s}^{-1}$ ) should exhibit an extremely large monopolar resonance, like air bubbles<sup>27</sup>, thereby causing the suspension to exhibit a negative effective bulk modulus  $B$ . These fairly dense particles should also exhibit a strong dipolar resonance, producing a negative effective mass density  $\rho$  in an overlapping frequency region. If they are considered as perfect (non-dissipative) media, such ‘double-negative acoustic metamaterials’ are expected to have negative acoustic indices<sup>24</sup>.

Such a straightforward analysis in terms of negative constitutive parameters may be inappropriate for a dissipative medium with a negative refractive index<sup>28</sup>. In both electromagnetism and acoustics, the refractive index  $n$  is complex-valued because it is defined as the ratio of the complex-valued wavenumber  $k$  ( $=\omega/\nu + j\alpha$ ) in the metamaterial to that in a reference medium  $k_0$  ( $=\omega/\nu_0 + j\alpha_0$ ), where  $\nu$  denotes the phase velocity,  $\alpha$  represents the attenuation coefficient and  $\omega$  is the angular frequency. For a non-dissipative reference medium ( $\alpha_0 = 0$ ), the refractive index  $n = \nu_0/\nu + j(\alpha\nu_0/\omega)$  is often referred to as its real part ( $=\nu_0/\nu$ ). By convention, its imaginary part is taken to be positive ( $\alpha > 0$ ), thus defining the forward direction along which the wave energy flows. Conventional dissipative media or positive-index materials support only forward wave motions ( $\nu > 0$ ). Metamaterials, however, can sustain backward waves ( $\nu < 0$ ) in the spectral vicinity of the particle resonances; such materials are referred to as negative-index materials<sup>1</sup>.

In this study, we exploited strong low-frequency Mie resonances of sub-wavelength macroporous silicone rubber microbeads to achieve negative-index metamaterials in the ultrasonic domain. We produced particles with a mean radius ( $\langle a \rangle$ ) of  $160 \mu\text{m}$  and a size dispersion of approximately 25% (Fig. 1a,b) by generating

<sup>1</sup>University of Bordeaux, CNRS, I2M-APY, UMR 5295, 33405 Talence, France. <sup>2</sup>University of Bordeaux, CNRS, CRPP, UPR 8641, 33600 Pessac, France.

<sup>3</sup>University of Bordeaux, CNRS, Solvay, LOF, UMR 5258, 33608 Pessac, France. \*e-mail: [thomas.brunet@u-bordeaux.fr](mailto:thomas.brunet@u-bordeaux.fr)

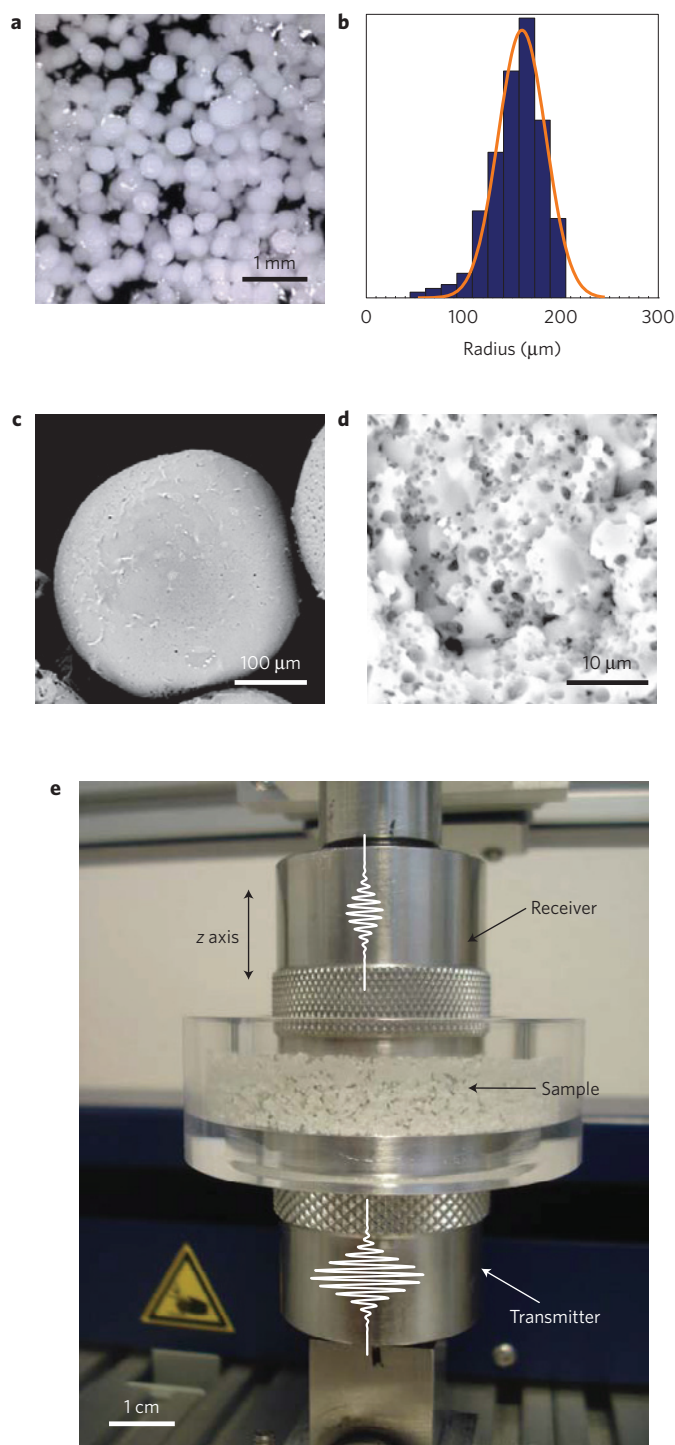


**Figure 1 | Soft 3D acoustic metamaterials composed of ultra-slow Mie resonators.** **a**, Optical microscopy image of macroporous silicone rubber microbeads embedded in a water-based gel matrix. **b**, Corresponding histogram showing the microbead size distribution. The mean radius ( $\langle a \rangle$ ) is 160  $\mu\text{m}$ , with the standard deviation  $\sigma$  of the distribution being 25%, as deduced from a Gaussian fit (solid line). The particle porosity is approximately 40%. **c,d**, Scanning electron microscope images of both the surface and core of a microbead, respectively. **e**, Photograph of the acoustical experimental set-up for the *in situ* measurements of phase velocity. The propagation distance  $z$  between the pair of large broadband ultrasonic transducers (emitter/receiver) could be varied precisely because the receiver was mounted on a  $z$  axis motorized linear stage.

high-internal-phase emulsion droplets in a simple microfluidic device<sup>29</sup>. These macroporous microbeads, with a porosity of approximately 40%, were then randomly dispersed in a water-based gel matrix—a Bingham fluid<sup>30</sup> that behaves acoustically like water ( $v_0 \approx 1,500 \text{ m s}^{-1}$ )—thus forming a concentrated suspension of ‘ultra-slow’ particles with a volume fraction  $\Phi_0$  of approximately 20%. Because the macroporous microbeads are closed (Fig. 1c), they are stable over time (a few days), unlike air bubbles (a few minutes), which are extremely sensitive to a variety of undesirable effects, such as Oswald ripening or dissolution in the host matrix<sup>31</sup>.

To determine the acoustic refractive index  $n$  of the investigated macroporous-particle suspensions, we measured the angular phase shifts of Gaussian pulses propagating through varying thicknesses in direct-acoustical-contact measurements (Fig. 1e). Ultrasonic pulses, with central frequencies  $f_0$  ranging from 50 kHz to 500 kHz, were emitted and detected using a pair of large broadband ultrasonic transducers (transmitter/receiver) of diameter 30 mm. Because the size of our macroporous particles is approximately 300  $\mu\text{m}$ —ten times smaller than the smallest incident wavelength used in our experiments (3 mm at 500 kHz for water)—our microbeads can be considered to be sub-wavelength resonators, as sought for metamaterials<sup>1</sup>. When the propagation distance  $z$  was varied from 1.0 mm to 1.5 mm, the transmitted temporal signals shifted on the time-delay axis, allowing us to directly infer the phase velocity  $v$  and the acoustic index  $n$  ( $=v_0/v$ ).

Indeed, such *in situ* acoustical measurements can avoid additional phase delays caused by the interfaces, as reported in electromagnetism<sup>6</sup>. Because the strong resonant scattering induces high attenuation in such a random medium, we detect only the ballistic coherent pulse<sup>32</sup>, which propagates from the transmitter to the receiver. Therefore, pulses reflected on the transducer surfaces are not propagated, thus avoiding spurious phase delays caused by interference between the successive echoes (Supplementary Information).

For all operating frequencies  $f_0$ , the amplitude of the transmitted pulses decreases when the propagation distance  $z$  is increased in such a passive medium, as illustrated at 140 kHz (Fig. 2a). However, the temporal shift of the pulse oscillations, which contains information regarding the phase velocity  $v$ , depends on the frequency  $f_0$ . Note that, in our conditions, by investigating ‘thin’ samples, we are able to infer the phase velocity unambiguously because the measured phase delays ( $\sim 0.1 \mu\text{s}$ ) are much smaller than the time period of the transmitted signals ( $> 1 \mu\text{s}$ ). Because all the oscillations shift as a whole, we focus our attention on the centre of the pulses, denoted by  $t_{\text{phase}}$  and for which the amplitude is zero, as depicted in Fig. 2b–d.

The forward shift of  $t_{\text{phase}}$  observed at 110 kHz (Fig. 2b) indicates a positive phase velocity (or positive acoustic index, Fig. 2e). By contrast, the backward shift of  $t_{\text{phase}}$  at 170 kHz (Fig. 2d) reveals a negative phase velocity (or negative acoustic index, Fig. 2g). For the intermediate frequency  $f_0 = 140 \text{ kHz}$ , the transmitted pulses are not shifted on the time-delay axis (Fig. 2c), indicating ‘infinite’ phase velocities (or zero acoustic index, Fig. 2f).

We also obtained the phase-velocity and acoustic-index spectra over a broad frequency range (50–500 kHz) from the angular-phase measurements performed on the fast Fourier transforms (FFTs) of the temporal signals recorded for two different propagation distances ( $z = 1.0 \text{ mm}$  and  $1.5 \text{ mm}$ ). The phase velocity  $v$  and the acoustic index  $n$  ( $=v_0/v$ ) were observed to be negative between 140 kHz and 275 kHz (see the black curves in Fig. 3a,b).

The initial sample ( $\Phi_0 \approx 20\%$ ) was then diluted to produce another sample with  $\Phi_1 \approx 15\%$ , which resulted in a clear reduction of the frequency width of the negative bands (red curves in Fig. 3a,b). When the volume fraction was drastically lowered ( $\Phi_2 \approx 0.2\%$ ), the negative features disappeared (green curves in Fig. 3a,b), giving

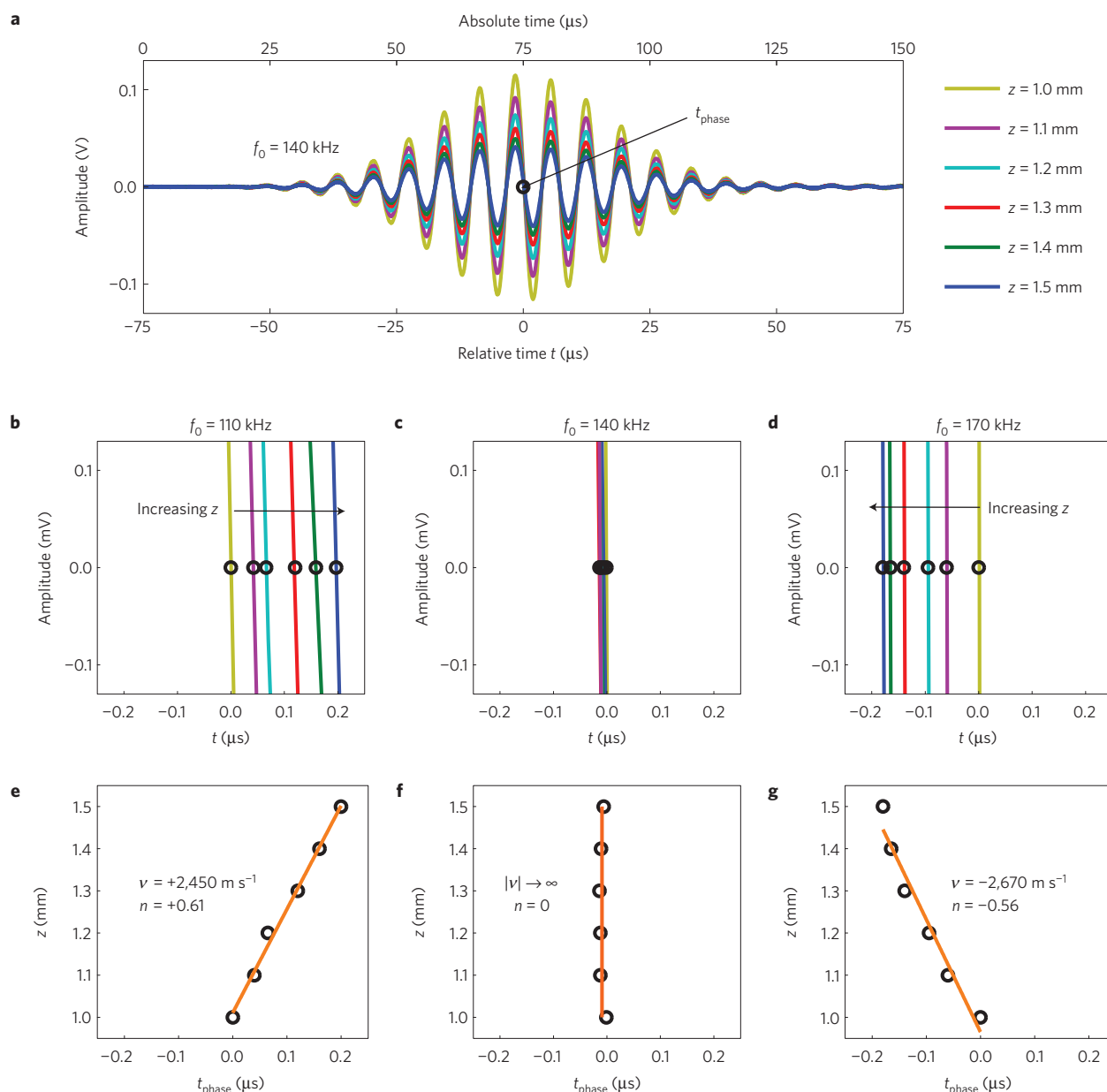


**Figure 2 | Phase delays of the transmitted signals as a function of propagation distance.** **a**, Examples of typical measured ballistic coherent pulses ( $f_0 = 140$  kHz) transmitted through a concentrated suspension of macroporous silicone rubber microbeads ( $\Phi_0 \approx 20\%$ ,  $\langle a \rangle = 160$  μm,  $\sigma = 25\%$ ) for six propagation distances  $z$  ( $= 1.0, 1.1, 1.2, 1.3, 1.4$  and  $1.5$  mm). The time  $t_{\text{phase}}$  refers to the centre of the pulses for which the amplitude is zero. **b–d**, Zoomed-in views of the oscillations around  $t_{\text{phase}}$  for  $f_0 = 110, 140$  and  $170$  kHz, respectively. **e–g**, Values of the time  $t_{\text{phase}}$  as a function of the propagation distance  $z$ , yielding experimental values for the phase velocity  $v$  ( $= \delta z / \delta t_{\text{phase}}$ ) and acoustic index  $n$  ( $= v_0 / v$ ) from linear regressions for  $f_0 = 110, 140$  and  $170$  kHz, respectively.

way to classical dispersion ( $v > 0$ ), as previously observed in bubbly media<sup>31</sup>.

Finally, we compared our acoustical measurements against theoretical predictions produced through multiple-scattering modelling, revealing fairly good qualitative agreement (Fig. 3a–d). To obtain the theoretical acoustic index  $n$ , we calculated the effective wavenumber  $k$  of our samples using the Waterman–Truell formula<sup>33</sup> (Supplementary Information), often used for concentrated random media ( $\Phi \approx 10\%$ ). The values of the parameters for the porous silicone rubber that were used for the calculations (the velocity and attenuation coefficient for both longitudinal and shear waves) were measured independently on large monolithic cylindrical samples (30 mm in diameter and

3 mm in thickness) of the same material as the microbeads. The material parameters used for the calculations are  $\rho_1 = 600$  kg m<sup>-3</sup>,  $v_L = 80$  m s<sup>-1</sup>,  $\alpha_L = 60$  Np mm<sup>-1</sup> MHz<sup>-1.5</sup> (for longitudinal waves) and  $v_T = 40$  m s<sup>-1</sup>,  $\alpha_T = 200$  Np mm<sup>-1</sup> MHz<sup>-1.5</sup> (for shear waves) for the porous silicone rubber and  $\rho_0 = 1,000$  kg m<sup>-3</sup>,  $v_0 = 1,500$  m s<sup>-1</sup> for the water-based gel matrix.

Through direct-pulse-propagation experiments on soft acoustic metamaterials, we confirmed that the phase velocity could be negative over a broad range of ultrasonic frequency bandwidths, thus demonstrating a three-dimensional negative-acoustic-index metamaterial. Our approach based on the use of soft-matter techniques means that these metafluids can be produced on a large scale, paving the way towards the production of acoustic devices

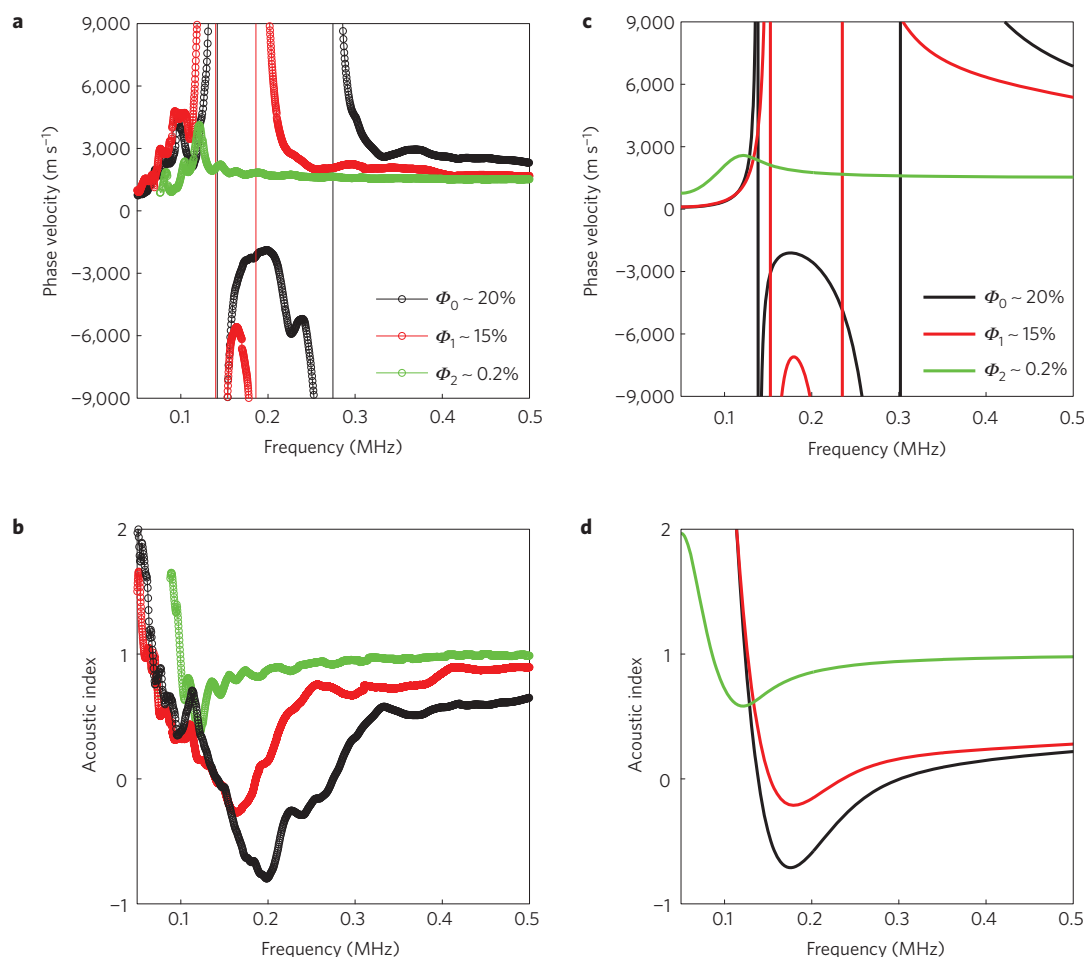


**Figure 3 | Comparisons between acoustical experiments and theoretical predictions.** **a**, Experimental phase velocities  $v$  extracted from fast Fourier transforms performed on ultrasonic Gaussian pulses with central frequencies  $f_0$  ranging from 50 kHz to 500 kHz. **b**, Experimental acoustic indices  $n (= v_0/v)$  deduced from the above phase-velocity spectra (**a**) given the knowledge of the phase velocity of the host matrix ( $v_0 \approx 1,500 \text{ m s}^{-1}$ ). **c,d**, Predicted phase velocities and acoustic indices, respectively, calculated in the framework of multiple scattering (see the Waterman-Truell formula given in the Supplementary Information). The volume fractions are approximately  $\Phi_0 \approx 20\%$  (black lines),  $\Phi_1 \approx 15\%$  (red lines) and  $\Phi_2 \approx 0.2\%$  (green lines).

with negative or zero-valued indices, as required for key applications such as sub-wavelength imaging and transformation acoustics.

Received 16 July 2014; accepted 4 November 2014;  
published online 15 December 2014

## References

1. Krowne, C. M. & Zong, Y. (eds) *Physics of Negative Refraction and Negative Index Materials* (Springer, 2007).
2. Cubukcu, E. *et al.* Electromagnetic waves: Negative refraction by photonic crystals. *Nature* **423**, 604–605 (2003).
3. Martinez-Sala, R. *et al.* Sound attenuation by sculpture. *Nature* **378**, 241 (1995).
4. Shelby, R. A., Smith, D. R. & Schultz, S. Experimental verification of a negative index of refraction. *Science* **292**, 77–79 (2001).
5. Zhang, S. *et al.* Experimental demonstration of near-infrared negative-index metamaterials. *Phys. Rev. Lett.* **95**, 137404 (2005).
6. Dolling, G. *et al.* Simultaneous negative phase and group velocity of light in a metamaterial. *Science* **312**, 892–894 (2006).
7. Soukoulis, C. M. & Wegener, M. Past achievements and future challenges in the development of three-dimensional photonic metamaterials. *Nature Photon.* **5**, 523–530 (2011).
8. Smith, D. R., Pendry, J. B. & Wiltshire, M. C. K. Metamaterials and negative refractive index. *Science* **305**, 788–792 (2004).
9. Wegener, M. Metamaterials beyond optics. *Science* **342**, 939–940 (2013).
10. Liu, Z. Y. *et al.* Locally resonant sonic materials. *Science* **289**, 1734–1736 (2000).
11. Lee, S. *et al.* Composite acoustic medium with simultaneously negative density and modulus. *Phys. Rev. Lett.* **104**, 054301 (2010).
12. Fok, L. & Zhang, X. Negative acoustic index metamaterial. *Phys. Rev. B* **83**, 214304 (2011).
13. Liang, Z. & Li, J. Extreme acoustic metamaterial by coiling up space. *Phys. Rev. Lett.* **108**, 114301 (2012).
14. Xie, Y. *et al.* Measurement of a broadband negative index with space-coiling acoustic metamaterials. *Phys. Rev. Lett.* **110**, 175501 (2013).
15. Pendry, J. B. Negative refraction makes a perfect lens. *Phys. Rev. Lett.* **85**, 3966–3999 (2000).
16. Kadic, M. *et al.* Metamaterials beyond electromagnetism. *Rep. Prog. Phys.* **76**, 126501 (2013).
17. Fang, N. *et al.* Ultrasonic metamaterials with negative modulus. *Nature Mater.* **5**, 452–456 (2006).
18. Li, J. *et al.* Experimental demonstration of an acoustic magnifying hyperlens. *Nature Mater.* **8**, 931–934 (2009).
19. Brunet, T., Leng, J. & Mondain-Monval, O. Soft acoustic metamaterials. *Science* **342**, 323–324 (2013).
20. Pendry, J. B. & Li, J. An acoustic metafluid: Realizing a broadband acoustic cloak. *New J. Phys.* **10**, 115032 (2008).
21. Norris, A. N. Acoustic metafluids. *J. Acoust. Soc. Am.* **125**, 839–849 (2009).
22. Seeman, R. *et al.* Droplet based microfluidics. *Rep. Prog. Phys.* **75**, 016601 (2012).
23. Brunet, T. *et al.* Tuning Mie scattering resonances in soft materials with magnetic fields. *Phys. Rev. Lett.* **111**, 264301 (2013).
24. Li, J. & Chan, C. T. Double-negative acoustic metamaterial. *Phys. Rev. E* **70**, 055602 (2004).
25. Still, T. *et al.* Soft silicone rubber in phononic structures: Correct elastic moduli. *Phys. Rev. B* **88**, 094102 (2013).
26. Allard, J.-F. *Propagation of Sound in Porous Media* (Springer, 1993).



27. Bretagne, A., Tourin, A. & Leroy, V. Enhanced and reduced transmission of acoustic waves with bubble meta-screens. *Appl. Phys. Lett.* **99**, 221906 (2011).
28. Dubois, J., Aristégui, C. & Poncelet, O. Spaces of electromagnetic and mechanical constitutive parameters for dissipative media with either positive or negative index. *J. Appl. Phys.* **115**, 024902 (2014).
29. Gokmen, M. & Du Prez, F. Porous polymer particles - A comprehensive guide to synthesis, characterization, functionalization and applications. *Prog. Polym. Sci.* **37**, 365–405 (2012).
30. Brunet, T. *et al.* Sharp acoustic multipolar-resonances in highly monodisperse emulsions. *Appl. Phys. Lett.* **101**, 011913 (2012).
31. Leroy, V. *et al.* Sound velocity and attenuation in bubbly gels measured by transmission experiments. *J. Acoust. Soc. Am.* **123**, 1931–1940 (2008).
32. Page, J. H. *et al.* Group velocity in strongly scattering media. *Science* **271**, 634–637 (1996).
33. Waterman, P. C. & Truell, R. Multiple scattering of waves. *J. Math. Phys.* **2**, 512–537 (1961).

## Acknowledgements

This work was supported by the Agence Nationale pour la Recherche (Grant 2011-BS0902101 Metakoustik-Aerospace Valley) and the US Air Force European Office of Aerospace Research and Development (Grant FA8655-12-1-2067).

This work was performed under the auspices of the Labex AMADEUS ANR-10-LABX-0042-AMADEUS with the help of French state Initiative d'Excellence IdEx ANR-10-IDEX-003-02. We thank G. Pibre from Bluestar Silicones for fruitful advice and providing us with the silicone rubber, and J. Valencony (Siltech Corp.) for the surfactants.

## Author contributions

T.B., O.M.-M., J.L., O.P. and C.A. designed the project. A.M. synthesized the macroporous soft silicone rubber microbeads with the help of K.Z. Formulation aspects were supervised by O.M.-M., A.M. set up the microfluidics with the advice of J.L., T.B. and B.M. conducted the acoustical measurements and performed the calculations under the guidance of C.A. and O.P. for the theoretical aspects. T.B. wrote the paper in collaboration with C.A., O.P., J.L. and O.M.-M.

## Additional information

Supplementary information is available in the [online version of the paper](#). Reprints and permissions information is available online at [www.nature.com/reprints](http://www.nature.com/reprints). Correspondence and requests for materials should be addressed to T.B.

## Competing financial interests

The authors declare no competing financial interests.